Femtosecond Solvation Dynamics in a Neat Ionic Liquid and Ionic Liquid Microemulsion: Excitation Wavelength Dependence

Aniruddha Adhikari, Kalyanasis Sahu, Shantanu Dey, Subhadip Ghosh, Ujjwal Mandal, and Kankan Bhattacharyya*

Department of Physical Chemistry, Indian Association for the Cultivation of Science, Jadavpur, Kolkata 700 032, India

Solvation dynamics in a neat ionic liquid, 1-pentyl-3-methyl-imidazolium tetra-flouroborate ([pmim][BF$_4$]) and its microemulsion in Triton X-100 (TX-100)/benzene is studied using femtosecond up-conversion. In both the neat ionic liquid and the microemulsion, the solvation dynamics is found to depend on excitation wavelength (λ_{ex}). The λ_{ex} dependence is attributed to structural heterogeneity in neat ionic liquid (IL) and in IL microemulsion. In neat IL, the heterogeneity arises from clustering of the pentyl groups which are surrounded by a network of cation and anions. Such a nanostructural organization is predicted in many recent simulations and observed recently in an X-ray diffraction study. In an IL microemulsion, the surfactant (TX-100) molecules aggregate in form of a nonpolar peripheral shell around the polar pool of IL. The micro-environment in such an assembly varies drastically over a short distance. The dynamic solvent shift (and average solvation time) in neat IL as well as in IL microemulsions decreases markedly as λ_{ex} increases from 375 to 435 nm. In a [pmim][BF$_4$]/water/TX-100/benzene quaternary microemulsion, the solvation dynamics is slower than that in a microemulsion without water. This is ascribed to the smaller size of the water containing microemulsion. The anisotropy decay in an IL microemulsion is found to be faster than that in neat IL.

1. Introduction

The room-temperature ionic liquids (RTILs) have been known for a very long time.[1] They are used extensively as an extraordinarily stable electrolyte for electrochemistry.[2] Interest in RTILs has been revived because of their recent applications as an environmentally benign ("green") solvent and catalyst for a host of organic recations.[3] A RTIL resembles a molten salt having bulky ions.[3] The steric hindrance of the bulky ions of a RTIL creates difficulty ("frustration") in crystal formation and gives rise to a low melting point. However, the interionic attractions in a RTIL cause high boiling point, very high viscosity (several hundred times that of water), and negligible vapor pressure.[4−7] A RTIL remains in the liquid phase over a wide range of temperature, is essentially nonvolatile, and is easily recyclable. Because of the presence of ions, an ionic liquid is quite polar. The polarity and solvation properties of the RTILs are addressed in several recent works.[4−6] Solvation dynamics in a RTIL occurs in a slow nanosecond time scale along with a subpicosecond component.[4−6] Recently, several groups carried out computer simulations on the structure and dynamics in a RTIL.[7] These simulations suggest that solvation dynamics in a RTIL involves collective motion of the cation and the anion.[7]

Very recently, many groups reported self-assembly of amphiphilic molecules in RTILs.[8−16] Petrich and co-workers studied solvation dynamics of coumarin 153 in amphiphilic ionic liquids, (1-cetyl-3-vinyl-imidazolium) bromide and 1-cetyl-3-vinyl-imidazolium bis-(trifluoro-methylsulfonyl)-imide, and their micelles in water.[8] They suggested that the imidazolium moiety is responsible for the major part of the solvation dynamics.[8] Sarkar and co-workers found that the average solvation time in

SCHEME 1: **Structure of (A) Coumarin 480 (C480) and (B) [pmim][BF$_4$]**
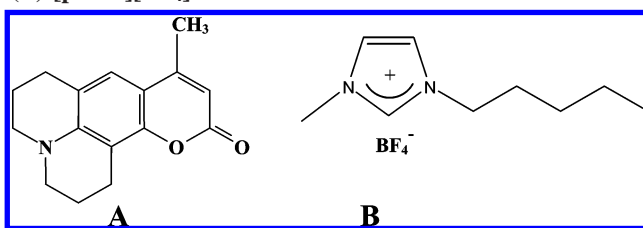
1-butyl-3-methyl-imidazolium hexafluorophospate, ([bmim]-[PF$_6$])/brij micelles is ∼3 ns.[14] The magnitude of retardation (∼2 times) of solvation dynamics for a micelle in a RTIL compared with that in a neat RTIL is much smaller than that (100−1000 times) observed in the case of a micelle in water.[16−20]

More recently, Gao et al. reported the formation of a microemulsion containing a nanosized pool of ionic liquid surrounded by a surfactant Triton X-100 (TX-100) in benzene[11a] and in cyclohexane.[11b−c] Using dynamic light scattering (DLS), they showed that the aggregates swell in size with increase in the mole ratio (R) of the polar phase (RTIL, [bmim][BF$_4$]) and the surfactant (TX-100).[11] At $R = 1$, they reported that the diameter of the microemulsion is 47 nm. Subsequently, Eastoe et al. carefully examined the structure of the same system using small angle neutron scattering (SANS).[12] They suggested formation of ellipsoidal droplets with a semi−minor radius 2.4 nm and length 11 nm at $R = 1.0$. They also found that the droplets are increasingly elongated with increase in R. The dimensions reported by Eastoe et al. are smaller than those reported by Gao et al. Most recently, Gao et al. studied effect of addition of water to [bmim][BF$_4$]/TX-100/benzene microemulsion.[11a] They reported that as much as 6 wt % water

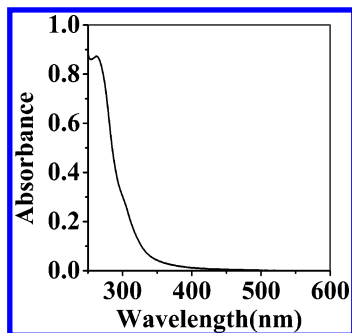* Corresponding author. E-mail: pckb@mahendra.iacs.res.in.

Figure 1. Absorption spectrum of neat [pmim][BF$_4$] (path length = 1 cm).
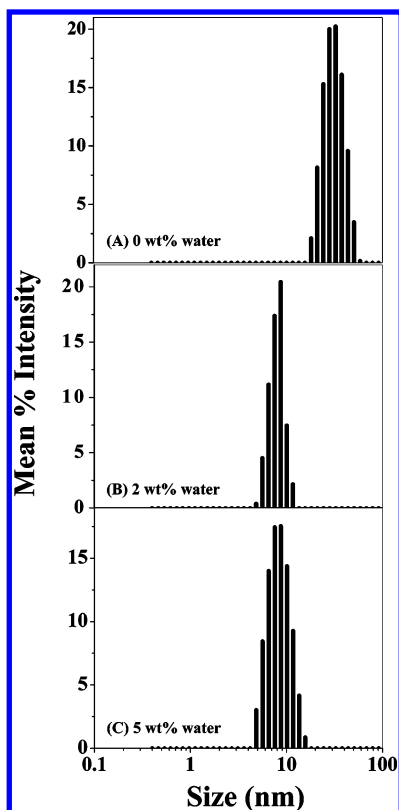

Figure 2. Size distribution of the droplets (measured by dynamic light scattring) in a microemulsion of [pmim][BF$_4$]/TX-100/benzene for R = 1.0 in the presence of (A) 0 wt %, (B) 2 wt %, and (C) 5 wt % water.

may be encapsulated in the polar nanodomain of the microemulsion. They, however, did not report the hydrodynamic diameter of the microemulsion in the presence of water. Sarkar and co-workers studied picosecond solvation dynamics in TX-100/[bmim][BF$_4$]/cyclohexane ternary microemulsion using C153 as the probe.[13−14] Owtrusky and co-workers studied ultrafast vibrational relaxation in ionic liquid microemulsions and found that the RTIL microemulsions are more polar than the neat RTILs.[15]

In the present work, we focus on a TX-100 based microemulsion containing the RTIL 1-pentyl-3-methyl-imidazolium tetra-flouroborate ([pmim][BF$_4$]). We first, study the formation of the microemulsion using dynamic light scattering and also using a fluorescence probe, coumarin 480 (C480). Second, we investigate the ultrafast solvation dynamics using femtosecond up-conversion. Finally, using excitation wavelength dependence, we spatially resolve the dynamics in different regions of the microemulsion and also in neat [pmim][BF$_4$].
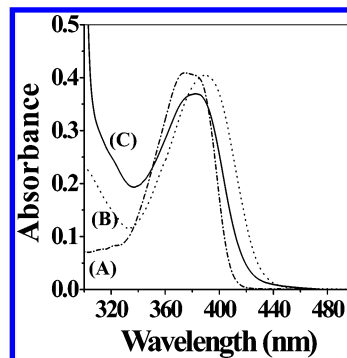

Figure 3. Absorption spectra of C480 in (A) benzene (dashed dotted), (B) neat [pmim][BF$_4$] (dotted), and (C) [pmim][BF$_4$]/TX-100/benzene microemulsion (R = 1.0) (solid line).
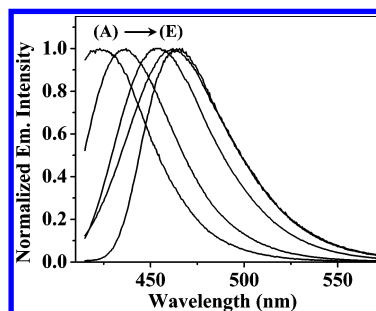

Figure 4. Emission spectra of C480 (λ_{ex} = 405 nm) in (A) benzene, (B) TX-100/benzene, (C) [pmim][BF$_4$]/TX-100/benzene microemulsion, (D) [pmim][BF$_4$]/TX-100/benzene microemulsion with 5 wt % water, and (E) neat [pmim][BF$_4$].

In a heterogeneous system (e.g., a microemulsion), a fluorescence probe may be distributed over a variety of locations ranging from a nonpolar region near the surfactants to a relatively more polar region at the core of the polar domain ("pool of ionic liquid"). The absorption and emission spectra of a solvation probe depend on the polarity of the medium. Thus, by varying the excitation wavelength (λ_{ex}), it is possible to excite the probe selectively at different locations. This is the basis of the so-called red edge excitation shift (REES) which is observed in many organized assemblies.[21−22] We have previously reported on λ_{ex} dependence of solvation dynamics in a microemulsion,[22a] a lipid vesicle,[22b] a micelle (triblock copolymer, P123),[22c] P123-SDS aggregate,[22d] and also on FRET in a microemulsion[22e] and a P123 gel.[22f] The λ_{ex} dependence has been attributed to the presence of the probes in different locations. We now study λ_{ex} dependence of solvation dynamics in a neat IL ([pmim][BF$_4$]) and its TX-100/benzene microemulsion.

According to many recent studies, neat ILs are heterogeneous.[23−27] The multiscale coarse grained simulation by Wang and Voth[23a] and atomistic simulations by Lopes and Padua[23b] predicted nanostructural organization in ionic liquids having alkyl chains longer or equal to C$_4$. The nanostructural organization involves clustering of the alkyl chains and formation of an ionic network comprising the cations and anions.[23] This leads to segregation of an ionic liquid into distinct polar and nonpolar domains.[23b] Several recent experiments confirm this prediction.[24−26] X-ray diffraction studies of alkyl(C$_n$)-methyl imidazolium [BF$_4$] reveals such structural organization in nanometer scale (13−27 Å for n = 4−10).[24] Optical heterodyne-detected Raman-induced Kerr effect studies (OHD-RIKES) provide further evidence in favor of such local structures in C5mim ILs.[25] Samanta and co-workers reported marked excitation wavelength dependence of steady-state emission spectra of several probes in IL.[4a,h,i] Recently, using MD simulations
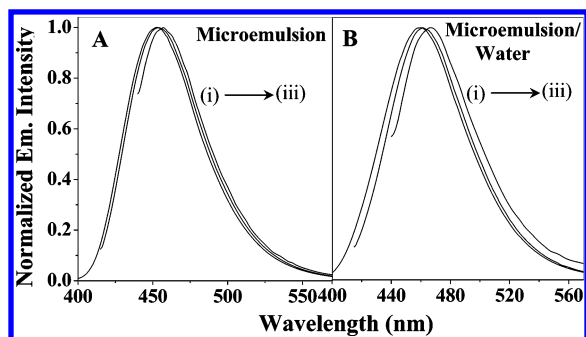
Femtosecond Solvation Dynamics

J. Phys. Chem. B, Vol. 111, No. 44, 2007 **12811**

Figure 5. Emission spectra of C480 in [pmim][BF$_4$]/TX-100/benzene microemulsion, (A) in the absence and (B) in the presence of 5 wt % water for (i) λ_{ex} = 375 nm, (ii) λ_{ex} = 405 nm, and (iii) λ_{ex} = 435 nm.

Hu and Margulis showed that REES in a RTIL arises from probes trapped in quasi-static solvent cages that relax in timescales longer than the fluorescence lifetime of the probes.[27] The dynamic aspect of REES in IL has not been investigated earlier. In this work, we show that solvation dynamics even in a neat IL depends on λ_{ex}. The heterogenieity in an IL microemulsion has a different origin. There are drastically different regions in an IL microemulsion ranging from a nonpolar one inside the alkyl chains of the surfactant to a polar region in the core of the pool of the IL.

2. Experimental Section

Laser grade coumarin 480 (C480, Exciton, Scheme 1A) was used as received. Sodium tetrafluoroborate (98%, Aldrich), 1-methylimidazole (99%, Aldrich), and 1-bromopentane (99%, Aldrich) were used for the synthesis of the room-temperature ionic liquid. Acetonitrile (Merck) was distilled over P$_2$O$_5$, and dichloromethane (Merck) was used as received. Diethyl ether (Merck) was distilled over KOH. TX-100 (Nacalai Tesque) was vacuum-dried for about 2 h before the experiments while benzene (UV grade, Spectrochem) was dried over sodium.

The IL, [pmim][Br] was prepared from 1-methylimidazole and 1-bromopentane following the sonochemical route as described by Namboodiri et al.[28a] Pure [pmim][BF$_4$] (Scheme 1B) was obtained through the metathesis of [pmim][Br] with NaBF$_4$ in dry acetonitrile under argon atmosphere at room temperature.[28b−c] For purification, the raw [pmim][BF$_4$] was diluted with dicholoromethane and filtered a couple of times through a silica gel column. The filtrate was treated with activated charcoal in an inert atmosphere for 48 h to remove any possible trace of color. After removal of dicholoromethane in a rotary evaporator, [pmim][BF$_4$] was repeatedly washed with dry diethyl ether to yield the RTIL in form of a colorless, viscous liquid.

The steady state absorption and emission spectra were recorded in a Shimadzu UV-2401 spectrophotometer and a Spex FluoroMax-3 spectrofluorimeter, respectively.

In our femtosecond upconversion setup (FOG 100, CDP), the sample was excited at 375, 405, and 435 nm using the second harmonic of a mode-locked Ti-sapphire laser (Tsunami, Spectra Physics), pumped by a 5 W Millennia (Spectra Physics). In order to generate second harmonic, we used a nonlinear crystal (1 mm BBO, θ = 25°, ϕ = 90°). The fluorescence emitted from the sample was upconverted in a nonlinear crystal (0.5 mm BBO, θ = 38°, ϕ = 90°) using the fundamental beam as a gate pulse. The upconverted light is dispersed in a monochromator and detected using photon counting electronics. A cross-correlation function obtained using the Raman scattering from ethanol displayed a full width at half-maximum (fwhm) of 350
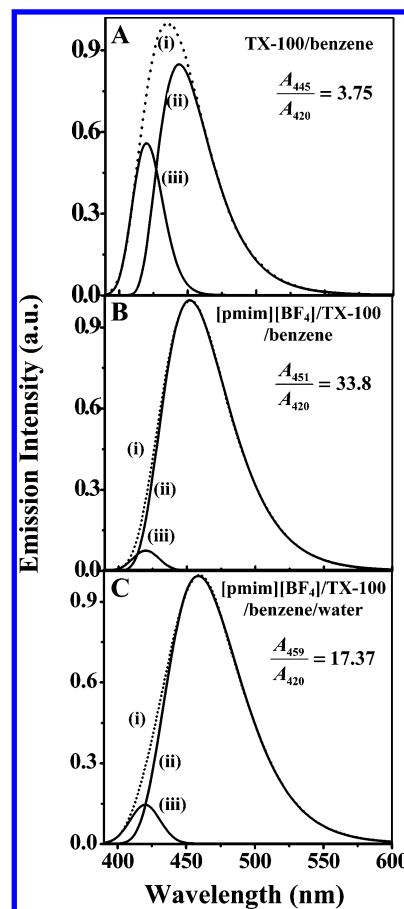

Figure 6. Decomposition of emission spectrum of C480 (λ_{ex} = 375 nm) into two spectra: in benzene and in polar pool of microemulsion. (i) Observed emission spectrum (dotted). (ii) Contribution of C480 in polar region (solid line). (iii) Contribution of C480 in bulk benzene (solid line) for (A) TX-100/benzene, (B) [pmim][BF$_4$]/TX-100/benzene microemulsion, and (C) [pmim][BF$_4$]/TX-100/benzene microemulsion with 5 wt % water. Ratios of the areas of emission specta in polar region to that in benzene are also indicated (A denotes area under curve with emission maxima mentioned as subscript).

fs. The femtosecond fluorescence decays were fitted using a Gaussian shape for the exciting pulse.

To fit the femtosecond data, one needs to know the long decay components. They were detected using a picosecond set up. For this purpose, the samples were excited at 375, 405, and 435 nm using picosecond diode lasers (IBH nanoleds) in an IBH Fluorocube apparatus. The emission was collected at a magic angle polarization using a Hamamatsu MCP photomultiplier (5000U-09). The time correlated single photon counting (TC-SPC) setup consists of an Ortec 9327 CFD and a Tennelec TC 863 TAC. The data is collected with a PCA3 card (Oxford) as a multichannel analyzer. The typical fwhm of the system response using a liquid scatterer is about 90 ps. The picosecond fluorescence decays were deconvoluted using IBH DAS6 software. All experiments were done at room temperature (293 K).

In order to fit the femtosecond transient, we first determined the long picosecond components by deconvolution of the picosecond decays. Then the long picosecond components were kept fixed to fit the femtosecond data. We have calculated emission frequency $\nu(t)$ up to ∼150 ps with the parameters obtained from the femtosecond data. After 150 ps, we used the $\nu(t)$ obtained from the picosecond TCSPC data.

The time-resolved emission spectra (TRES) were constructed using the parameters of best fit to the fluorescence decays and

TABLE 1: Anisotropy Decay of C480 in [pmim][BF₄]/TX-100/benzene Microemulsion (λ_ex = 405 nm) as a Function of R = [RTIL]/[TX-100]

R	r_0	$\tau_{r1}(a_1)$ (ps)	$\tau_{r2}(a_2)$ (ps)	$\langle\tau_r\rangle_{av}$,[a] (ps)
0	0.21	180		180
0.5	0.28	180 (75%)	700 (25%)	300
1.0	0.33	180 (65%)	700 (35%)	350

[a] ± 10%, $\langle\tau_r\rangle_{av} = a_1\tau_{r1} + a_2\tau_{r2}$.

TABLE 2: λ_ex Dependence of Anisotropy Decay of C480 in [pmim][BF₄]/TX-100/benzene Microemulsion (R = 1.0)

water (wt %)	λ_{ex}	r_0	$\tau_{r1}(a_1)$ (ps)	$\tau_{r2}(a_2)$ (ps)	$\langle\tau_r\rangle_{av}$[a] (ps)
0	375	0.28	180 (85%)	700 (15%)	250
	405	0.33	180 (65%)	700 (35%)	350
	435	0.34	180 (38%)	700 (62%)	500
5	375	0.30	180 (90%)	800 (10%)	250
	405	0.27	180 (71%)	800 (29%)	350
	435	0.29	180 (28%)	800 (72%)	600

[a] ± 10%, $\langle\tau_r\rangle_{av} = a_1\tau_{r1} + a_2\tau_{r2}$.

TABLE 3: Decay Parameters of C(t) of C480 in Neat [pmim][BF₄] at Different λ_ex

λ_{ex} (nm)	$\Delta\nu_{obs}$[a] (cm⁻¹)	$\tau_i(a_i)$ (ps)	$\langle\tau_s\rangle$[c] (ps)
375	925	≤0.3 (16%)[b], 2 (4%), 250 (46%), 2200 (34%)	860
405	625	≤0.3 (42%)[b], 2 (3%), 250 (26%), 2200 (28%)	680
435	335	≤0.3 (67%)[b], 2 (4%), 250 (4%), 500 (25%)	135

[a] ± 50 cm⁻¹. [b] Calculated using the Fee−Maroncelli method.[29b] [c] ± 10%, $\langle\tau_s\rangle = \Sigma a_i\tau_i$.

the steady-state emission spectrum following the procedure described by Maroncelli and Fleming.[29a] The solvation dynamics is described by the decay of the solvent correlation function $C(t)$, defined as,

$$C(t) = \frac{\nu(t) - \nu(\infty)}{\nu(0) - \nu(\infty)} \quad (1)$$

where $\nu(0)$, $\nu(t)$, and $\nu(\infty)$ are the emission maxima (frequencies) at time 0, t, and ∞, respectively. Note, a portion of solvation dynamics is missed even in our femtosecond set up of time resolution 350 fs. The amount of solvation missed is calculated using the Fee−Maroncelli procedure.[29b] The emission frequency at time zero, $\nu^p_{em}(0)$, may be calculated using the absorption frequency (ν^p_{abs}) in a polar medium (i.e., C480 in [pmim][BF₄]) as,[29b]

$$\nu^p_{em}(0) = \nu^p_{abs} - (\nu^{np}_{abs} - \nu^{np}_{em}) \quad (2)$$

where ν^{np}_{em} and ν^{np}_{abs} denote the steady-state frequencies of emission and absorption, respectively, of the probe (C480) in a nonpolar solvent (i.e., cyclohexane).

In order to study fluorescence anisotropy decay, the analyzer was rotated at regular intervals to get perpendicular ($I_\perp$) and parallel ($I_\parallel$) components. Then the anisotropy function, $r(t)$ was calculated using the formula

$$r(t) = \frac{I_\parallel(t) - GI_\perp(t)}{I_\parallel(t) + 2GI_\perp(t)} \quad (3)$$

The G value of the picosecond set up was determined using a probe whose rotational relaxation is very fast, for example, coumarin 480 in methanol, and the G value was found to be 1.5.

The dynamic light scattering studies were carried out in a NanoZS instrument (Malvern, U.K.) using a 5 mW He−Ne laser (632 nm).

3. Results and Discussions

3.1. Purity and Absorption Spectrum of Neat [pmim]-[BF₄]. A key issue in any study on RTIL is the purity of the RTILs. We have very carefully purified the RTIL and checked the purity using absorption spectroscopy. The absorption spectrum of the RTIL [pmim][BF₄] is shown in Figure 1. Previously, it was reported that [bmim][BF₄] shows a peak[13c]

or a prominent shoulder[4e] at ~350 nm. We did not observe either the shoulder or the peak at 350 nm. Our purified RTIL sample exhibited negligible absorbance at a wavelength >350 nm (e.g., OD ~ 0.01 in a 1 cm cell at 405 nm).

3.2. Absorption and Emission Spectra of C480 in Neat [pmim][BF₄]. In neat [pmim][BF₄], C480 shows an absorption maximum at 390 nm, which is blue-shifted by 6 nm from that in water (396 nm)[30] and is close to that reported for ethanol (387 nm).[30]

C480 exhibits intense fluorescence with emission maximum at ~462 nm in neat [pmim][BF₄]. The emission maximum of C480 in neat [pmim][BF₄] does not change with variation of excitation wavelength (λ_{ex}). We have recently observed that, in a P123-SDS aggregate although the observed REES is small, the λ_{ex} dependence on solvation is quite pronounced.[22d] In section 3.6, we show that solvation dynamics in neat [pmim]-[BF₄] displays appreciable dependence on λ_{ex}.

3.3 Dynamic Light Scattering and Formation of [pmim]-[BF₄]/ TX-100/Benzene Microemulsion. Dynamic light scattering of a mixture of TX-100 and [pmim][BF₄] in benzene indicates formation of microemulsion. The results are shown in Figure 2. At a [pmim][BF₄]/ TX-100 molar ratio, $R = 1.0$, the average hydrodynamic diameter is found to be 31.8 nm. This is larger than the hydrodynamic diameter of a TX-100 reverse micelle (~4 nm) in benzene.[31] The larger droplet (microemulsion) size for the [pmim][BF₄]/TX-100/benzene system suggests formation of a polar domain ("pool") containing the RTIL.

On addition of water, the droplet size of [pmim][BF₄]/TX-100/water/benzene system decreases (diameter 9.3 nm at 2 wt % and 8.5 nm at 5 wt % water). However, the water containing microemulsions are still larger than the TX-100 reverse micelle (diameter ~4 nm). In the following section, we show that the emission spectrum of a probe C480 also indicates formation of a microemulsion.

3.4. Absorption and Emission Spectra of C480 in [pmim]-[BF₄]/TX-100/Benzene Microemulsion: λ_ex Dependence. The absorption spectra of C480 in benzene and in [pmim][BF₄]/TX-100/benzene microemulsion are shown in Figure 3.

In benzene, the emission maximum of C480 is at 420 nm (Figure 4). On addition of TX-100 to a solution of C480 in benzene, the emission maximum of C480 exhibits a marked red shift to 435 nm (Figure 4). The marked red shift by 15 nm indicates transfer of the C480 molecules from bulk benzene to the interior of TX-100 reverse micelle. On addition of the RTIL ([pmim][BF₄]) to the TX-100/benzene reverse micelle, the emission maximum of C480 displays a further red shift by 18 nm to 453 nm (at $\lambda_{ex} = 405$ nm, Figure 4). The red shift suggests formation of a microemulsion in which the probe C480 is located inside the polar domain ("pool" of the RTIL). Note, the emission maximum of C480 in the microemulsion is different from that (462 nm) in neat [pmim][BF₄] (Figures 4 and 5).

Figure 5A describes the λ_{ex} dependence of the emission spectrum of C480 in [pmim][BF₄]/TX-100/benzene microemul-

Femtosecond Solvation Dynamics

J. Phys. Chem. B, Vol. 111, No. 44, 2007 **12813**

TABLE 4: Decay Parameters of $C(t)$ of C480 in [pmim][BF$_4$]/TX-100/benzene Microemulsions in the Absence and Presence of 5 wt % Water at Different λ_{ex}

water (wt %)	λ_{ex} (nm)	$\Delta\nu_{obs}{}^a$ (cm^{-1})	$\tau_i(a_i)$ (ps)	$\langle\tau_s\rangle^c$ (ps)
0	375	1255	2 (19%), 200 (15%), 2200 (66%)	1480
	405	1025	≤0.3 (17%)^b, 2 (22%), 200 (12%), 2200 (49%)	1100
	435	235	≤0.3 (79%)^b, 2 (5%), 200 (16%)	30
5	375	1670	2 (10%), 250 (13%), 2200 (77%)	1725
	405	1490	≤0.3 (3%)^b, 2 (4%), 250 (35%), 2200 (58%)	1360
	435	500	≤0.3 (65%)^b, 2 (7%), 250 (12%), 500 (16%)	110

^{a} ±50 cm^{-1}. ^{b} Calculated using Fee-Maroncelli Method.[29b] ^{c} ± 10%, $\langle\tau_s\rangle = \Sigma a_i\tau_i$.

sion. It is apparent that inside the microemulsion there is a marked red shift of emission maximum of C480 with increase in λ_{ex}. The emission maxima of C480 are at 451, 453, and 457 nm respectively for $\lambda_{ex} = 375$, 405, and 435 nm (Figure 5A). The REES (i.e., λ_{ex} dependence of emission maximum) suggests that C480 molecules are distributed over a variety of locations inside the microemulsion. The very small emission intensity of C480 at 420 nm in the case of [pmim][BF$_4$]/TX-100/benzene microemulsion (at $\lambda_{ex} = 375-435$ nm) suggests that very few C480 molecules reside in bulk benzene and almost all of them are encapsulated inside the polar domain containing the RTIL. Obviously, excitation at a short wavelength ("blue edge") selects the probe in a relatively less polar region near the surfactant (TX-100). Excitation at a red end selects the probe molecules in a polar region inside the core of the pool containing RTIL.

The effect of addition of water on the emission spectrum of C480 in [pmim][BF$_4$]/TX-100 RTIL microemulsion is shown in Figure 5B. On addition of water, the emission maximum exhibits a further red shift. In 5 wt % water, the emission maximum of C480 is found to be red-shifted by ∼8 nm from that in a microemulsion without water. This suggests that addition of water increases polarity of the pool.

In order to estimate contribution of the emission spectrum of the probe (C480) in benzene (bulk), we decomposed the observed emission spectra (Figures 4 and 5) in the microemulsion as a sum of emission spectrum of C480 in benzene (bulk) and in the polar region (IL or water pool) of the microemulsion. The results are shown in Figure 6. From Figure 6 it is readily seen that in the micro-emulsion the contribution of the polar region (IL or water pool) are 97% and 95%, respectively. Thus, the contribution of C480 in benzene to the steady-state emission spectrum in the micro-emulsion is <5%, and at long emission wavelengths (450−550 nm), the contribution of emission of C480 in benzene is negligible. Further, the coumarin dyes display very fast solvation dynamics in neat benzene with average solvation time 0.78 ps.[32] If the ultrafast part of the dynamics were due to C480 in benzene, its contribution would have decreased with increase in excitation wavelength (since absorption spectrum of C480 in benzene is blue-shifted from that in the micro-emulsion, Figure 3). The results show the exactly opposite trend (contribution of ultrafast portion increased with increase in excitation wavelength, Table 4). Therefore, we do not believe that the observed excitation wavelength dependence is due to contribution of C480 in benzene.

3.5. Fluorescence Anisotropy Decay of C480 in [pmim]-[BF$_4$]/TX-100/Benzene Microemulsion: λ_{ex} Dependence. In bulk water, the time constant of fluorescence anisotropy decay of C480 is ∼70 ps.[33] In neat ([pmim][BF$_4$]), C480 exhibits a very slow rotational dynamics (Figure 7) with a single-exponential decay of time constant, 3800 ± 200 ps. The slow anisotropy decay in neat ionic liquid may obviously be ascribed to the high viscosity of ([pmim][BF$_4$]).[4−6]

The anisotropy decay of C480 in TX-100/benzene is found to be quite fast with a time constant of 180 ps ($\lambda_{ex} = 405$ nm, Figure 8, Table 1). On addition of the ionic liquid [pmim][BF$_4$] to the TX-100/benzene reverse micelle, the anisotropy decay of C480 slows down markedly with the emergence of an additional slow (700 ps) component (Figure 8, and Table 1). This suggests that within the RTIL containing microemulsion, there are two broadly different regions: a fast region near the head group of TX-100 of rotational relaxation time 180 ps and a slow region of rotational relaxation time ∼700 ps at the pool of the RTIL. The average rotational time is found to be 180, 300, and 350 ps for $R = 0$, 0.5, and 1.0 respectively, ($R =$ [RTIL]/[TX-100]). It is interesting to note that both the components of rotational relaxation in the RTIL containing microemulsion are faster than that in neat [pmim][BF$_4$]. This indicates lower microscopic friction in the pool of the RTIL compared with the neat RTIL, [pmim][BF$_4$].

Figure 9 and Table 2 describe λ_{ex} dependence of the anisotropy decay of C480 in [pmim][BF$_4$]/TX-100/benzene microemulsion. With increase in λ_{ex}, relative contribution of the fast (180 ps) component of anisotropy decay decreases from 85% at $\lambda_{ex} = 375$ nm to 38% at $\lambda_{ex} = 435$ nm with a concomitant increase in the contribution of the slow (700 ps) component from 15% to 62%. As a result, with increase in λ_{ex} from 375 to 435 nm, the average rotational relaxation time increases twofold. The average rotational times are 250, 350, and 500 ps for $\lambda_{ex} = 375$, 405, and 435 nm, respectively (Table 2).

The λ_{ex} dependence of anisotropy decay in the [pmim][BF$_4$] microemulsion may be explained as follows. With rise in λ_{ex}, a more polar region of the microemulsion (i.e., the "pool" of RTIL) is selected. In a RTIL based microemulsion, the viscosity inside the nanoscopic polar pool of RTIL is higher than that at the interface (because of the high viscosity of RTIL). This causes a slow down of the anisotropy decay and an increase in the average rotational relaxation time with increase in λ_{ex}.

Similar λ_{ex} dependence is also observed in the case of water containing [pmim][BF$_4$]/TX-100/benzene microemulsion (Table 2). In this case, for all λ_{ex}, the anisotropy decay is described by two time constants 180 and 800 ps. The contribution of the 800 ps component increases from 10% at $\lambda_{ex} = 375$ nm to 72% at $\lambda_{ex} = 435$ nm, and the average rotational relaxation time increases from 250 to 600 ps.

3.6. Solvation Dynamics in Neat [pmim][BF$_4$]: λ_{ex} Dependence. In neat [pmim][BF$_4$] for all λ_{ex}, the fluorescence decays of C480 exhibit a decay at the blue end and a rise at the red end. This is typical of a probe undergoing solvation dynamics. The solvation dynamics of C480 in neat [pmim][BF$_4$] is found to depend on λ_{ex}. The decay of $C(t)$ in neat [pmim]-[BF$_4$] at various λ_{ex} are shown in Figure 10, and the decay parameters are listed in Table 3. For $\lambda_{ex} = 375$ nm, the decay of $C(t)$ exhibits an average solvation time of 860 ps (Table 3). With increase in λ_{ex}, the average solvation time decreases about
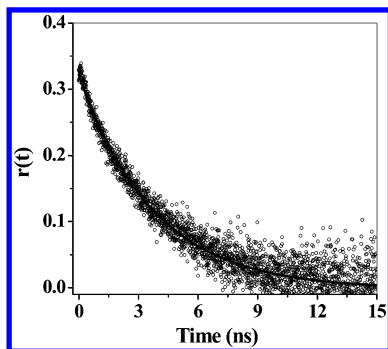
Figure 7. Fluorescence anisotropy decay of C480 (λ_{em} = 445 nm) along with a fitted curve in neat [pmim][BF$_4$] at λ_{ex} = 405 nm.
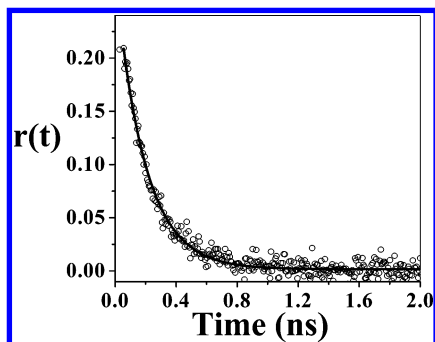

Figure 8. Fluorescence anisotropy decay of C480 (λ_{em} = 430 nm) along with fitted curve in TX-100/benzene at λ_{ex} = 405 nm.
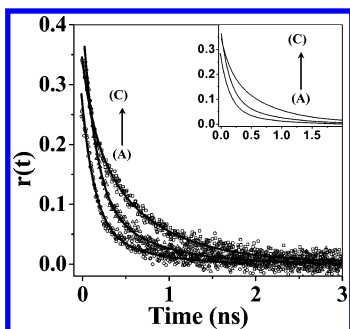

Figure 9. Fluorescence anisotropy decays of C480 (λ_{em} = 445 nm) along with fitted curves in [pmim][BF$_4$]/TX-100/benzene microemulsion (R = 1.0) at (A) λ_{ex} = 375 nm (○), (B) λ_{ex} = 405 nm (△), and (C) λ_{ex} = 435 nm (□). Initial part of the fitted curves are shown in the inset.

6 times to 135 ps at λ_{ex} = 435 nm. The total dynamic solvent shift is found to be 925, 625, and 335 cm^{-1} respectively for λ_{ex} = 375, 405, and 435 nm (Table 3).

Maroncelli and co-workers studied solvation dynamics of C153 and 4-AP in many ionic liquids using a picosecond set up (resolution ~25 ps).[5a,e] In butyl-methyl-imidazolium-[BF$_4$], they reported a total dynamic solvent shift of 900−1000 cm^{-1} for λ_{ex} near the absorption maxima of the probes (C153 and 4-AP). When we excited the probe (C480) near the absorption maximum (~375 nm), we detected a total dynamic solvent shift of 925 cm^{-1} in neat pentyl-methyl-imidazolium-[BF$_4$]. Considering that our probe (C480) and the RTIL (pentyl group) are slightly different, we feel our results are consistent with those of Maroncelli and co-workers for λ_{ex} near the absorption maximum of the probe. However, when λ_{ex} is shifted toward the red, we observed significant differences from the results reported by Maroncelli group. For λ_{ex} = 405 and 435 nm, we detected a total dynamic solvent shift of respectively 625 cm^{-1} and 335 cm^{-1}, which are significantly smaller than that (925 cm^{-1}) at λ_{ex} = 375 nm. Further, for these λ_{ex}'s we detected significant amount of ultrafast component (2 ps and <0.3 ps).
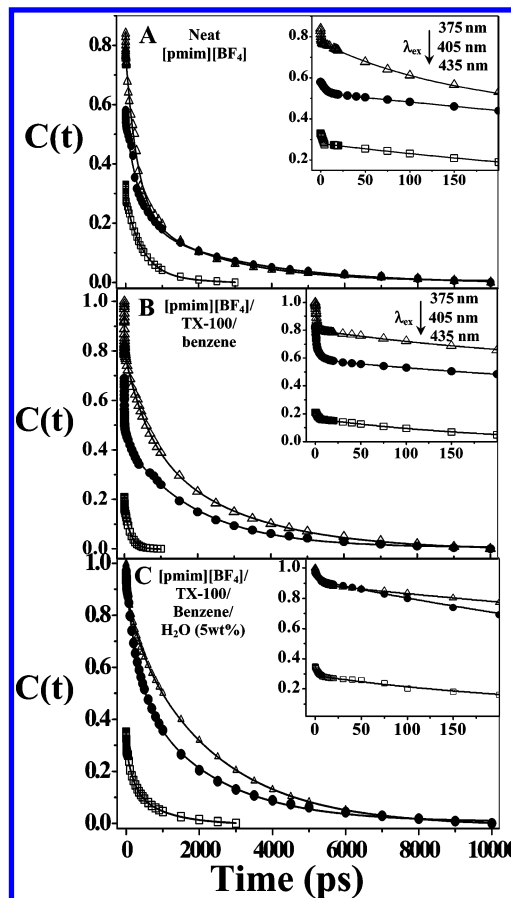

Figure 10. Decay of the solvent response function, $C(t)$ of C480: (A) in neat [pmim][BF$_4$]; (B) in [pmim][BF$_4$]/TX-100/benzene reverse micelle; (C) in [pmim][BF$_4$]/TX-100/benzene/water microemulsion for λ_{ex} = 375 nm (△), λ_{ex} = 405 nm (●), and λ_{ex} = 435 nm (□). The points denote the actual values of $C(t)$, and the solid lines denote the best fit.

The contribution of the ultrafast component is 45% at λ_{ex} = 405 nm and 71% at λ_{ex} = 435 nm (Table 3). The average solvation time decrease about 6 times from 860 ps at λ_{ex} = 375 nm to 135 ps at λ_{ex} = 435 nm. The λ_{ex} dependence of solvation dynamics suggests the presence of heterogeneity even in a neat ionic liquid. This is consistent with recent simulations,[23,27] X-ray diffraction,[24] and OHD-RIKES study,[25] on ionic liquids as discussed earlier.

It may be mentioned that Maroncelli and co-workers recently reported that in a set up of 100 fs time resolution 10−20% of solvation is missed in [bmim] [BF$_4$] when trans-4-dimethyl-amnio-4′-cyanostilbene is used as a probe.[5b] According to a recent simulation by Kobrak,[7a] in a RTIL, only ~15% of the solvation dynamics occurs in <5 ps. It is clear that for excitation near the peak of the probe (~at λ_{ex} = 375 nm for C480) our results are consistent with the simulations carried out by Kobrak. However, for excitation of the probe (C480) near the red end of its absorption spectra (λ_{ex} = 405 and 435 nm), the contributions of the ultrafast component (<5 ps) detected in our work are much larger (respectively, 42% and 66%) than that (~15%) predicted by Kobrak.

One possible reason for the discrepancy is the nanostructural organization in neat IL[23−27] which Kobrak did not take into account in their simulation. It may be pointed out that several recent simulations predict a large contribution of ultrafast solvation dynamics.[7b,c] For instance, Jeong et al.[7b] introduced effect of solute polarizability in the simulations and found that ~50% of the solvent relaxation occurs in subpicosecond time

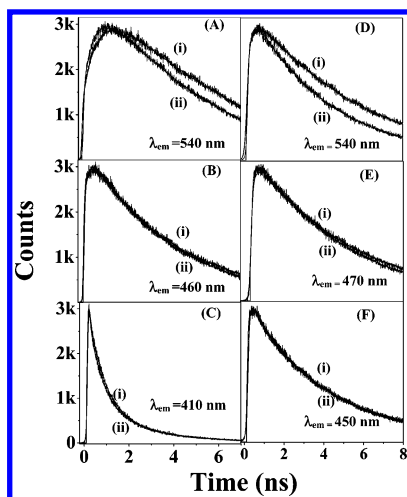**Figure 11.** Picosecond decay of the C480 in [pmim][BF$_4$]/TX-100/benzene microemulsion at λ_{ex} = 375 nm (A–C) and 435 nm (D–F); λ_{em} at (A) 540 nm, (B) 460 nm, (C) 410 nm, (D) 540 nm, (E) 470 nm, and (F) 450 nm. (i) In the presence and (ii) in the absence of 5 wt % water.
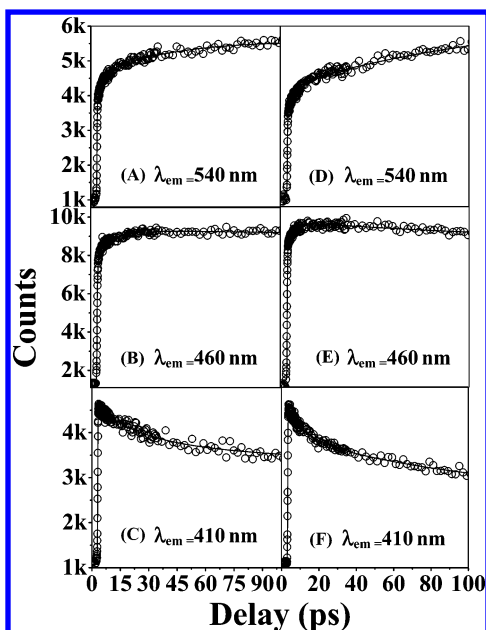

Figure 12. Femtosecond transient of the C480 in [pmim][BF$_4$]/TX-100/benzene microemulsion at λ_{em} (A) 540 nm, (B) 460 nm, (C) 410 nm, (D) 540 nm, (E) 460 nm, and (F) 410 nm. In the absence (A–C) and presence (D–F) of 5 wt % water (λ_{ex} = 375 nm).

scale. It seems simulations which consider the structural heterogeneity of the ionic liquid and other factors (e.g., solute polarizability) may explain the results reported in the present study.

3.7. Solvation Dynamics in [pmim][BF$_4$]/TX-100/Benzene Microemulsion: λ_{ex} Dependence. Solvation dynamics of C480 in the [pmim][BF$_4$]/TX-100/benzene microemulsion exhibits stronger λ_{ex} dependence compared with neat RTIL, [pmim]-[BF$_4$]. Figures 11 and 12 show the picosecond and femtosecond fluorescence transients of C480 in this microemulsion. Figure 13 shows the time-resolved emission spectra (TRES). The decays of $C(t)$ for the microemulsion at different λ_{ex} are shown in Figure 10, and the decay parameters are summarized in Table 4.

It is readily seen that, in [pmim][BF$_4$]/TX-100/benzene microemulsion with rise in λ_{ex}, the solvation dynamics (i.e., decay of $C(t)$) become faster. The observed λ_{ex} and, hence,
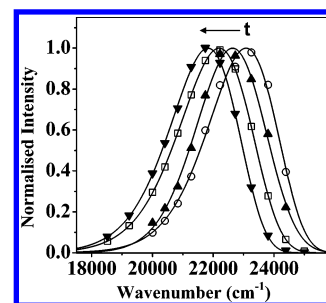

Figure 13. Time-resolved emission spectra (TRES) of C480 in [pmim]-[BF$_4$]/TX-100/benzene microemulsion at λ_{ex} = 375 nm at time (A) 0 ps (○), (B) 200 ps (▲), (C) 1500 ps (□), and (D) 10000 ps (▼).

location dependence of solvation dynamics in [pmim][BF$_4$]/TX-100/benzene system are similar to those observed earlier in the case of a water-in-oil microemulsion[22e] and other organized assemblies.[22]

In the case of the [pmim][BF$_4$]/TX-100/benzene microemulsion, for all λ_{ex}, $C(t)$ is fitted to a triexponential: a very slow (2200 ps) component, and a slow (200 ps) and a very fast 2 ps component. Apart from this, there is an ultrafast component (<0.3 ps) which is missed even in our femtosecond set up. The different components may originate from different regions of the microemulsion. The 2200 ps component may be assigned to the highly constrained region in the interior of the surfactant, while the 200 ps may be ascribed to the interface region near the polar head groups of TX-100. The ultrafast components (<0.3 and 2 ps) may arise from the core of the ionic liquid pool where the mobility of particularly the counterion is very fast. In the [pmim][BF$_4$]/TX-100/benzene microemulsion, contribution of the ultrafast components (<0.3 and 2 ps) increases from 19% at λ_{ex} = 375 nm to 84% at λ_{ex} = 435 nm, and the average solvation time decreases ~50-fold from 1480 ps at λ_{ex} = 375 nm to 30 ps at λ_{ex} = 435 nm.

Addition of water to the [pmim][BF$_4$]/TX-100/benzene microemulsion results in slightly slower solvation dynamics (longer $\langle \tau_s \rangle$ at all λ_{ex} (Table 4)). In this case, the solvation dynamics is described by 3 components: a very slow 2200 ps component inside the surfactants, a 250 ps component at the interface between TX-100 and the polar "pool", and a ultrafast component (2 ps and <0.3 ps) at the core of the pool (of IL and water). Contribution of the ultrafast component (2 ps and <0.3 ps) increases from 10% at λ_{ex} = 375 nm to 72% at λ_{ex} = 435 nm (Table 4). The average solvation time decreases about 16 times from 1725 to 110 ps. It may be noted that the solvation dynamics in water containing [pmim][BF$_4$]/TX-100/benzene microemulsion is slower compared with that without water. This may be attributed to the smaller size of the "pool" water containing microemulsion (diameter ~ 9 nm) compared with the large (31.8 nm) microemulsion without water. In the smaller water containing microemulsion, the distance of the polar entities (water and RTIL) from the head group of the surfactant (TX-100) is shorter, and this makes the dynamics slower.

4. Conclusion

This work reports on the excitation wavelength dependence of the solvation dynamics and anisotropy decay in neat [pmim]-[BF$_4$] and its microemulsion. The excitation wavelength dependence is attributed to the presence of heterogeneity. In neat ionic liquid, the heterogeneity may arise from nanostructural organization and existence of distinctly different microenvironments in neat ionic liquid. In a microemulsion, the local structure varies rapidly from the surfactant to the polar domain ("pool"),

and this seems to be the major source of excitation wavelength dependence. Addition of water to the microemulsion is found to slow down the solvation dynamics in the microemulsion. This has been ascribed to the smaller size of the water containing microemulsions. The anisotropy decay of C480 inside a microemulsion is found to be faster compared with that in neat [pmim][BF$_4$].

References and Notes

(1) (a) Hurley, F. H.; Wier, T. P. *J. Electrochem. Soc.* **1951**, *98*, 203. (b) Wilkes, J. S. *Green Chem.* **2002**, *4*, 73.

(2) (a) Kornyshev, A. A. *J. Phys. Chem. B* **2007**, *111*, 5545. (b) Buzzeo, M. C.; Evans, R. G.; Compton, R. G. *Chem. Phys. Chem.* **2004**, *5*, 1106. (c) Bonhote, P.; Dias, A.-P.; Papageorgiou, N.; Kalyansundram, K.; Gratzel, M. *Inorg. Chem.* **1996**, *35*, 1168.

(3) (a) Zhang, Z. C. *Adv. Catalysis* **2006**, *49*, 153. (b) Rogers, R. D.; Seddon, K. R. *Science* **2003**, *302*, 792. (c) Dupont, J.; de Souza, R. F.; Suarez, P. A. Z. *Chem. Rev.* **2002**, *102*, 3667.

(4) (a) Samanta, A. *J. Phys. Chem. B* **2006**, *110*, 13704. (b) Pal, A.; Samanta, A. *J. Phys. Chem. B* **2007**, *111*, 4724. (c) Karmakar, R.; Samanta, A. *J. Phys. Chem. A* **2002**, *106*, 6670. (d) Karmakar, R.; Samanta, A. *J. Phys. Chem. A* **2002**, *106*, 4447. (e) Paul, A.; Mandal, P. K.; Samanta, A. J. *Phys. Chem. B* **2005**, *109*, 9148. (f) Mandal, P. K.; Paul, A.; Samanta, A. *Res. Chem. Int.* **2005**, *31*, 575. (g) Aki, S. N. V. K.; Brennecke, J. F.; Samanta, A. *Chem. Commun.* **2001**, 413. (h) Mandal, P. K.; Sarkar, M.; Samanta, A. *J. Phys. Chem. A* **2004**, *108*, 9048. (i) Mandal, P. K.; Paul, A.; Samanta, A. *J. Photochem. Photobiol. A* **2006**, *182*, 113.

(5) (a) Jin, H.; Baker, G. A.; Arzhantsev, S.; Dong, J.; Maroncelli, M. *J. Phys. Chem. B* **2007**, *111*, 7291. (b) Arzhantsev, S.; Jin, H.; Baker, G. A.; Maroncelli, M. *J. Phys. Chem. B* **2007**, *111*, (c) Ito, N.; Arzhantsev, S.; Heitz, M.; Maroncelli, M. *J. Phys. Chem. B* **2004**, *108*, 5771. (d) Ito, N.; Arzhantsev, S.; Maroncelli, M. *Chem. Phys. Lett.* **2004**, *396*, 83. (e) Ingram, J. A.; Moog, R. S.; Ito, N.; Biswas, R.; Maroncelli, M. *J. Phys. Chem. B* **2003**, *107*, 5926.

(6) (a) Funston, A. M.; Fadeeva, T. A.; Wishart, J. F.; Castner, E. W., Jr. *J. Phys. Chem. B.* **2007**, *111*, 4963. (b) Shirota, H.; Castner, E. W., Jr. *J. Phys. Chem. A* **2005**, *109*, 9388.

(7) (a) Kobrak, M. N. *J. Chem. Phys.* **2006**, *125*, 064502. (b) Jeong, D.; Shim, Y.; Choi, M. Y.; Kim, H. J. *J. Phys. Chem. B* **2007**, *111*, 4920. (c) Bhargava, B. L.; Balasubramanian, S. *J. Chem. Phys.* **2006**, *125*, 219901. (d) Huang, X. H.; Margulis, C. J.; Li, Y. H.; Berne, B. J. *J. Am. Chem. Soc.* **2005**, *127*, 17842. (e) Liu, X.; Zhou, G.; Zhang, S.; Wu, G.; Yu, G. *J. Phys. Chem. B* **2007**, *111*, 5658. (f) Ghatee, M. H.; Ansari, Y. *J. Chem. Phys.* **2007**, *126*, 154502.

(8) (a) Chowdhury, P. K.; Halder, M.; Sanders, L.; Calhoun, T.; Anderson, J. L.; Armstrong, D. W.; Petrich, J. W. *J. Phys. Chem. B* **2004**, *108*, 10245. (b) Mukherjee, P.; Crank, J. A.; Halder, M.; Armstrong, D. W.; Petrich, J. W. *J. Phys. Chem. A* **2006**, *110*, 10725.

(9) (a) Anderson, J. L.; Pino, V.; Hagberg, E. C.; Sheares, V. V.; Armstrong, D. W. *Chem. Commun.* **2003**, 2444. (b) Fletcher, K. A.; Pandey, S. *Langmuir* **2004**, *20*, 33. (c) Yoshoi, M.; Mukai, T.; Kanie, K.; Yoshizawa, M.; Ohno, H.; Kato, T. *Adv. Mater.* **2002**, *14*, 351.

(10) (a) Wang, L.; Chen, X.; Chai, Y.; Hao, J.; Sui, Z.; Zhuang, W.; Sun, Z. *Chem. Commun.* **2004**, 2840. (b) Bowlas, C. J.; Bruce, D. W.; Seddon, K. R. *Chem. Commun.* **1996**, 1625.

(11) (a) Gao, Y.; Li, N.; Zheng, L.; Bai, X.; Yu, L.; Zhao, X.; Zhang, J.; Zhao, M.; Li, Z. *J. Phys. Chem. B* **2007**, *111*, 2506. (b) Gao, Y.; Han, S.; Han, B.; Li, G.; Shen, D.; Li, Z.; Du, J.; Hou, W.; Zhang, G. *Langmuir* **2005**, *21*, 5681. (c) Gao, H.; Li, J.; Han, B.; Chen, W. L.; Zhang, J.; Zhang, R.; Yan, D. *Phys. Chem. Chem. Phys.* **2004**, *6*, 2914. (d) Gao, Y.; Li, N.; Zheng, L.; Zhao, X.; Zhang, J.; Cao, Q.; Zhao, M.; Li, Z.; Zhang, G. *Chem.—Eur. J.* **2007**, *13*, 2661.

(12) Eastoe, J.; Gold, S.; Rogers, S. E.; Paul, A.; Welton, T.; Heenan, R. K.; Grillo, I. *J. Am. Chem. Soc.* **2005**, *127*, 7302.

(13) (a) Chakraborty, A.; Seth, D.; Chakrabarty, D.; Setua, P.; Sarkar, N. *J. Phys. Chem. A* **2005**, *109*, 11110. (b) Seth, D.; Chakraborty, A.; Setua, P.; Sarkar, N. *Langmuir* **2006**, *22*, 7768. (c) Supporting information of ref. 13a. (d) Seth, D.; Chakraborty, A.; Setua, P.; Sarkar, N. *J. Phys. Chem. A* **2007**, *111*, 4781.

(14) Seth, D.; Chakraborty, A.; Setua, P.; Sarkar, N. *J. Phys. Chem. B* **2007**, *111*, 4781.

(15) (a) Sando, G.; Dahl, K.; Owrutsky, J. C. *J. Phys. Chem. B* **2007**, *111*, 4901. (b) Sando, G. M.; Dahl, K.; Owrutsky, J. C. *Chem. Phys. Lett.* **2006**, *418*, 402.

(16) (a) Bagchi, B. *Chem. Rev.* **2005**, *105*, 3197. (b) Bhattacharyya, K. *Acc. Chem. Res.* **2003**, *36*, 95.

(17) (a) Correa, N. M.; Levinger, N. E. *J. Phys. Chem. B* **2005**, *110*, 13050. (b) Baruah, B.; Roden, J. M.; Sedgwick, M.; Correa, N. M.; Crans, D. C.; Levinger, N. E. *J. Am. Chem. Soc.* **2006**, *128*, 12758.

(18) (a) Harpham, M. R.; Ladanyi, B. M.; Levinger, N. E. *J. Phys. Chem. B* **2005**, *109*, 16891. (b) Faeder, J.; Ladanyi, B. M. *J. Phys. Chem. B* **2005**, *109*, 6732. (c) Thompson, W. H. *J. Chem. Phys.* **2004**, *120*, 8125. (d) Gomez, J. A.; Thompson, W. H. *J. Phys. Chem. B* **2004**, *108*, 20144. (e) Senapati, S.; Berkowitz, M. L. *J. Chem. Phys.* **2003**, *118*, 1937.

(19) (a) Balasubramanian, S.; Pal, S.; Bagchi, B. *Phys. Rev. Lett.* **2002**, *89*, 115505. (b) Pal, S.; Balasubramanian, S.; Bagchi, B. *J. Phys. Chem. B* **2003**, *107*, 5194. (c) Pal, S.; Bagchi, B.; Balasubramanian, S. *J. Phys. Chem. B* **2005**, *109*, 12879.

(20) Sterpone, F.; Marchetti, G.; Pierleoni, C.; Marchi, M. *J. Phys. Chem. B* **2006**, *110*, 11504.

(21) (a) Demchenko, A. P. *Biophys. Chem.* **1982**, *15*, 101. (b) Lakowicz, J. R. *Biochemistry* **1984**, *23*, 3013. (c) Mukherjee, S.; Chattopadhyay, A. *Langmuir* **2005**, *21*, 287.

(22) (a) Satoh, T.; Okuno, H.; Tominaga, K.; Bhattacharyya, K. *Chem. Lett.* **2004**, *33*, 1090. (b) Sen, P.; Satoh, T.; Bhattacharyya, K.; Tominaga, K. *Chem. Phys. Lett.* **2005**, *411*, 339. (c) Sen, P.; Ghosh, S.; Sahu, K.; Mondal, S. K.; Bhattacharyya, K. *J. Chem. Phys.* **2006**, *124*, 204905. (d) Mandal, U.; Adhikari, A.; Dey, S.; Ghosh, S.; Mondal, S. K.; Bhattacharyya, K. *J. Phys. Chem. B* **2007**, *111*, 5896. (e) Mondal, S. K.; Ghosh, S.; Sahu, K.; Mandal, U.; Bhattacharyya, K. *J. Chem. Phys.* **2006**, *125*, 224710. (f) Ghosh, S.; Dey, S.; Adhikari, A.; Mandal, U.; Bhattacharyya, K. *J. Phys. Chem. B* **2007**, *111*, 7085.

(23) (a) Wang, Y.; Voth, G. A. *J. Am. Chem. Soc.* **2005**, *127*, 12192. (b) Lopes, J. N. A. C.; Padua, A. A. H. *J. Phys. Chem. B* **2006**, *110*, 3330.

(24) Triolo, A.; Russina, O.; Bleif, H.-J.; Di Cola, E. *J. Phys. Chem. B* **2007**, *111*, 4641.

(25) Xiao, D.; Rajian, J. R.; Cady, A.; Li, S.; Bartsch, R. A.; Quitevis, E. L. *J. Phys. Chem. B* **2007**, *111*, 4669.

(26) Shigeto, S.; Hamaguchi, H. *Chem. Phys. Lett.* **2006**, *427*, 329.

(27) Hu, Z.; Margulis, C. J. *Proc. Natl. Acad. Sci. U.S.A.* **2006**, *103*, 831.

(28) (a) Namboodiri, V. V.; Varma, R. S. *Org. Lett.* **2002**, *4*, 18, 3161. (b) Ding, S.; Radosz, M.; Shen, Y. *Macromolecules* **2005**, *38*, 5921. (c) Dupont, J.; Consorti, C. S.; Suarez, P. A. Z.; de Souza, R. F. *Org. Synthesis* **2004**, *10*, 184.

(29) (a) Maroncelli, M.; Fleming, G. R. *J. Chem. Phys.* **1987**, *86*, 6221. (b) Fee, R. S.; Maroncelli, M. *Chem. Phys.* **1994**, *183*, 235.

(30) Jones, G., II; Jackson, W. R.; Choi, C.-Y.; Bergmark, W. R. *J. Phys. Chem.* **1985**, *89*, 294.

(31) (a) Zhu, D.-M.; Wu, X.; Schelly, Z. A. *J. Phys. Chem.* **1992**, *96*, 7121. (b) Zhu, D.-M.; Wu, X.; Schelly, Z. A. *Langmuir* **1992**, *8*, 1538. (c) Zhu, D.-M.; Wu, X.; Schelly, Z. A. *J. Phys. Chem.* **1992**, *96*, 2382. (d) Zhu, D.-M.; Wu, X.; Schelly, Z. A. *Langmuir* **1992**, *8*, 48. (e) Caldaru, H.; Caragheorgheopal, A.; Dimonie, M.; Donescu, D.; Dragutan, I.; Marinescu, N. *J. Phys. Chem.* **1992**, *96*, 7109. (f) Dutt, G. B. *J. Phys. Chem. B* **2004**, *108*, 7944.

(32) Luther, B. M.; Kimmel, J. R.; Levinger, N. E. *J. Chem. Phys.* **2002**, *116*, 3370.

(33) Shirota, H.; Segawa, H. *J. Phys. Chem. A* **2003**, *107*, 3719.